Electronic Supplementary Material (ESI) for Soft Matter.

Supplementary Information for: Glass transition of ion-containing polymer melts in bulk and thin films

Wei Li[†] and Monica Olvera de la Cruz[*,†,‡,¶,§]

†*Department of Materials Science and Engineering, Northwestern University, Evanston, IL 60208*

‡*Department of Physics and Astronomy, Northwestern University, Evanston, IL 60208*

¶*Department of Chemistry, Northwestern University, Evanston, IL 60208*

§*Department of Chemical and Biological Engineering, Northwestern University, Evanston, IL 60208*

E-mail: m-olvera@northwestern.edu

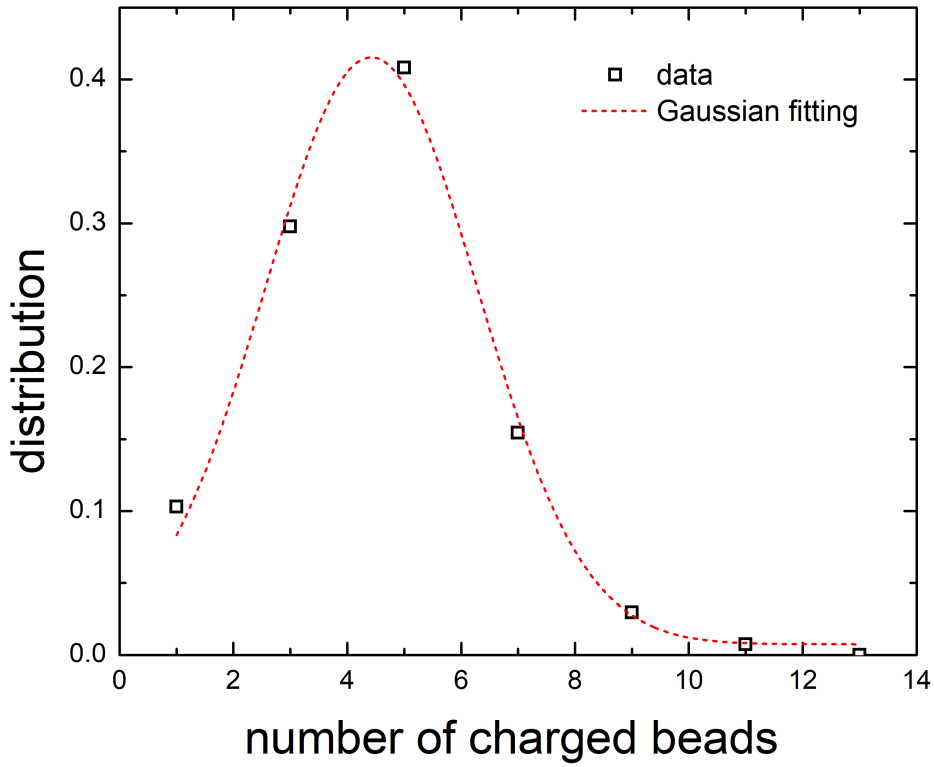

Figure S1: Distribution of the number of charged beads per chain for random ionic polymers of charge fraction $f_c = 0.1$. The fitting by a Gaussian distribution function yields a width of 1.866, close to the expected value of $[f_c(1 - f_c)N]^{1/2} \approx 1.897$ where chain length $N = 40$.

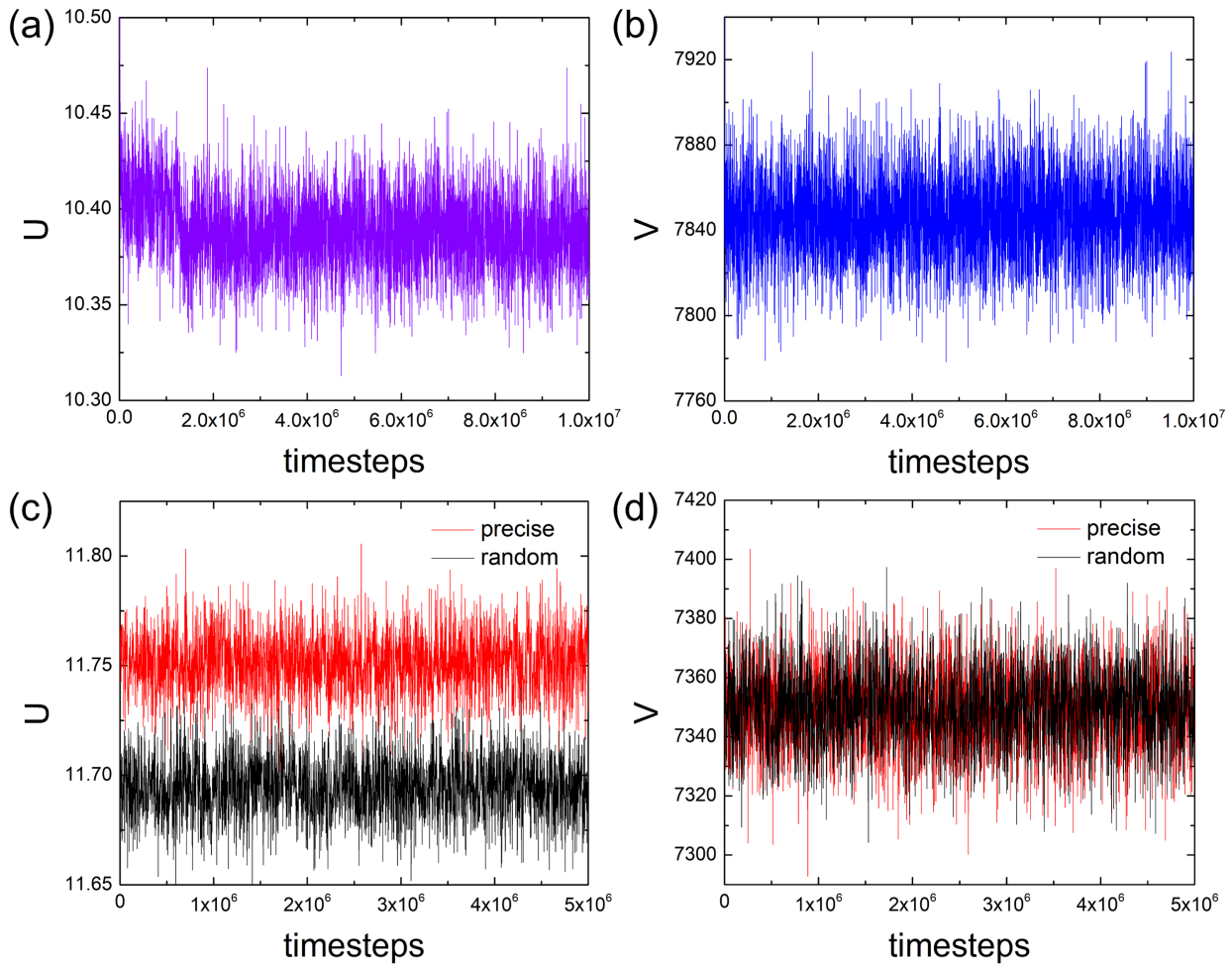

Figure S2: Temporal evolution of (a) total potential energy U and (b) simulation box volume V of bulk precise ionic polymers at $f_c = 0.1$, $l_B = 22.4$, and $T = 1.0$ in the initial equilibration run; (c) U and (d) V in the production run for bulk random and precise ionic polymers at $f_c = 0.1$, $l_B = 5.6$, and $T = 0.7$.

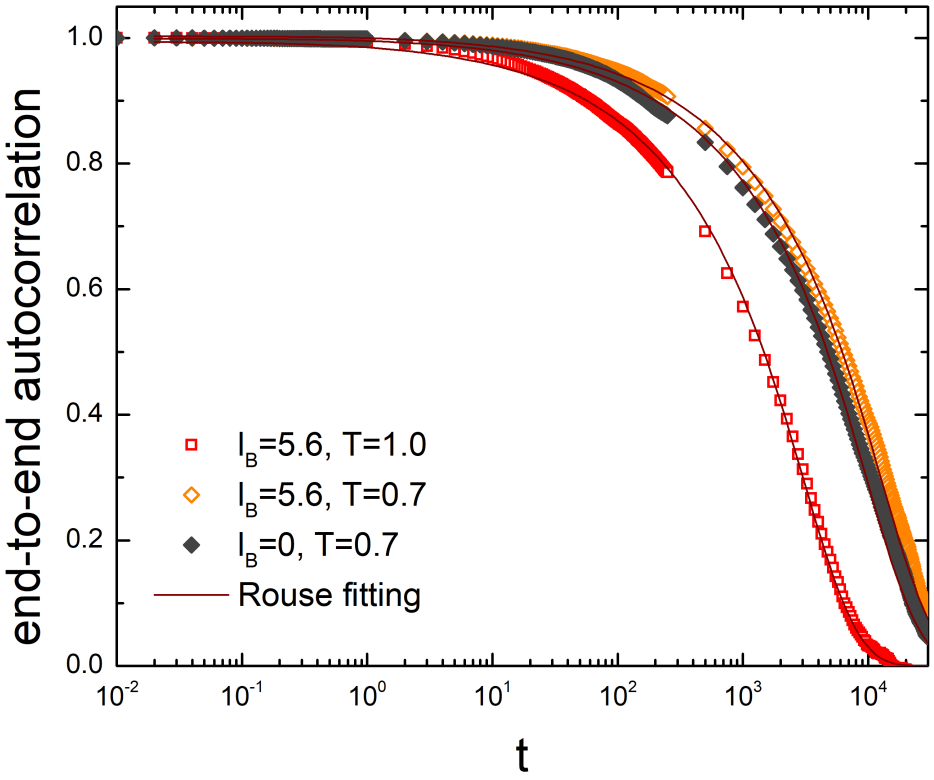

Figure S3: End-to-end vector autocorrelation functions along with time for bulk random ionic polymers of $f_c = 0.1$ at different l_B and T, where $l_B = 0$ indicates the neutral system without electrostatic interactions. Solid lines show fitting by the Rouse model, suggesting good agreement of chain dynamics with the Rouse model prediction at high temperatures. The fitted Rouse time is $\tau_R = 9684.595$ for $l_B = 0$ and $T = 0.7$, $\tau_R = 12604.299$ and 3039.416 for $l_B = 5.6$ at $T = 0.7$ and 1.0, respectively.

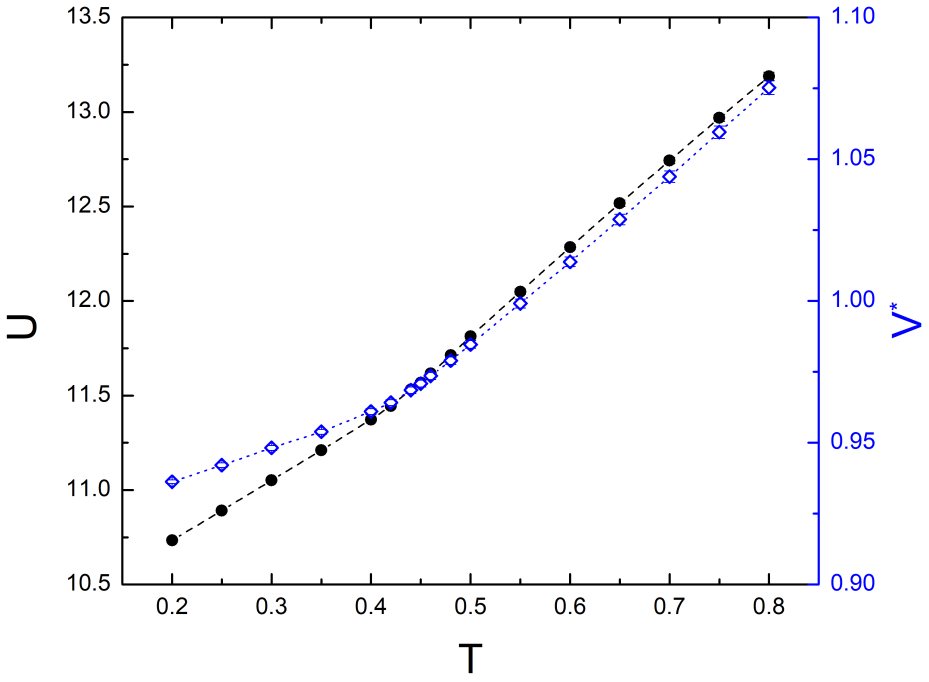

Figure S4: Plot of total energy U and specific volume V^* as a function of temperature T for bulk random ionic polymers of $f_c = 0.1$ and $l_B = 5.6$, whereas the V^* profile shows a larger change in slopes around the transition.

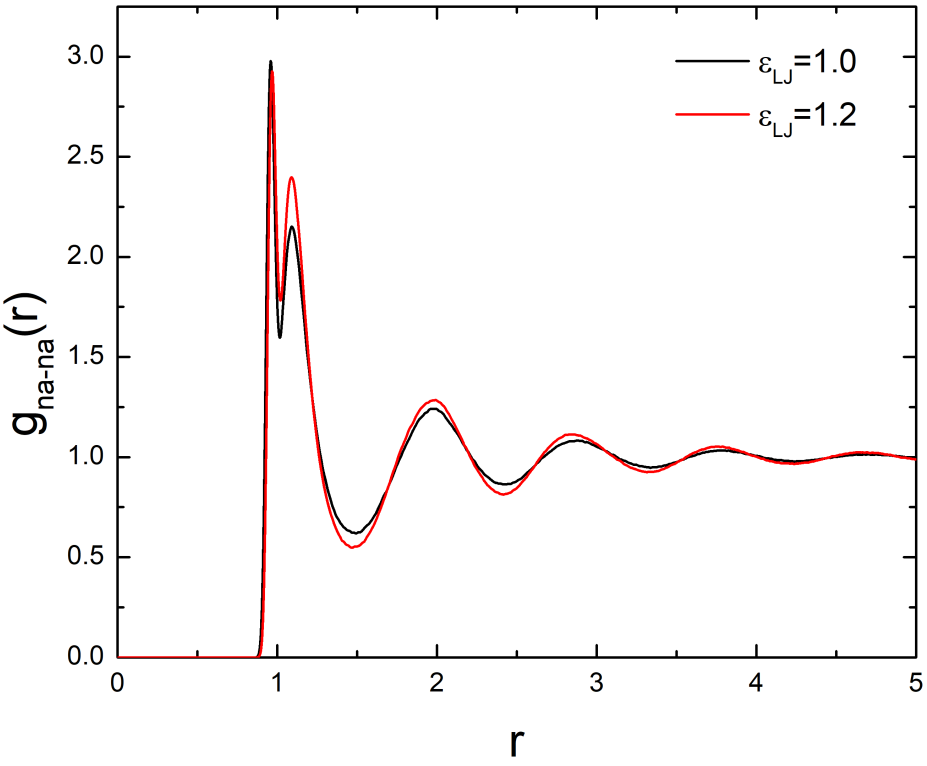

Figure S5: Radial distribution function of polymer beads for bulk neutral systems ($l_B = 0$ and $f_c = 0.1$) of $T = 0.7$ at $\epsilon_{LJ} = 1.0\epsilon$ and 1.2ϵ.

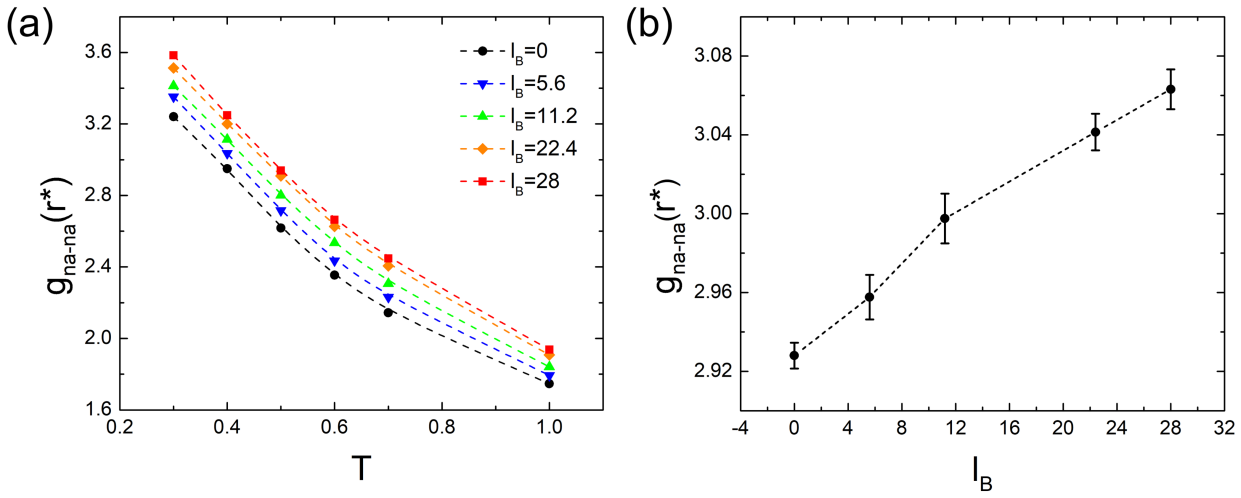

Figure S6: (a) Height of nearest neighbor peak (at peak position r^*) in the radial distribution function of neutral beads, $g_{\text{na-na}}(r^*)$, as a function of T at different l_B for bulk random ionic polymers of $f_c = 0.1$. (b) $g_{\text{na-na}}(r^*)$ at the glass transition for different l_B, extracted from the interpolation of the plots in (a) at T_g.

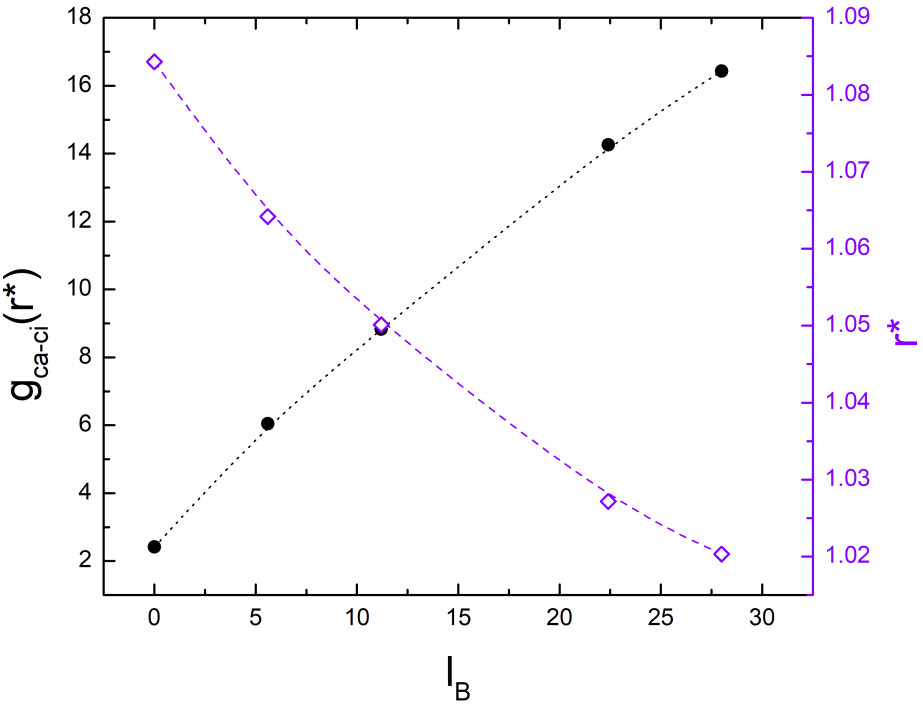

Figure S7: Primary peak height and position of radial distribution function between charge beads and counterions, $g_{\text{ca-ci}}(r)$, as a function of l_B.

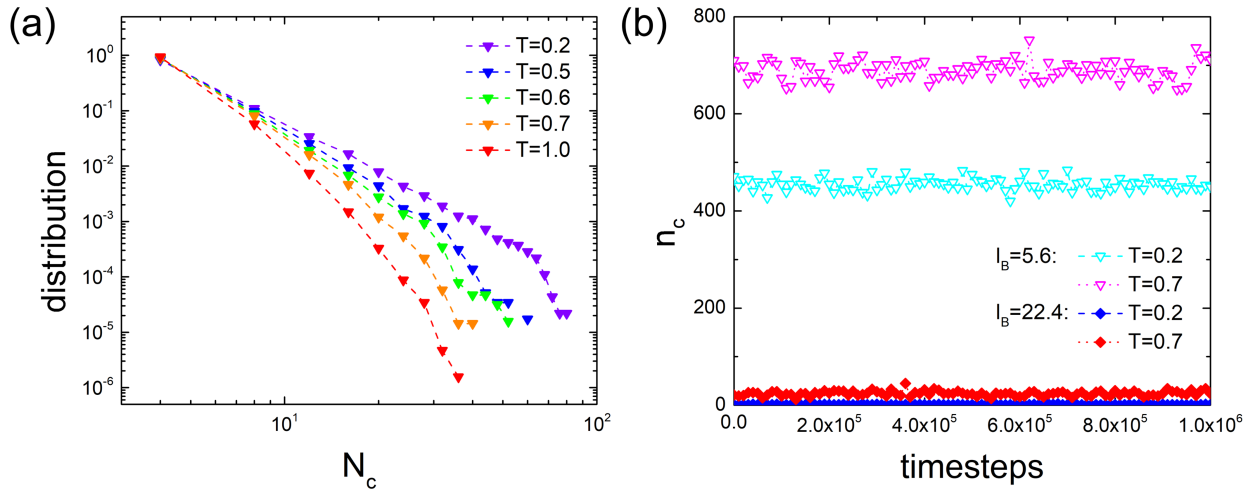

Figure S8: (a) Distribution of ionic cluster size N_c at different T for bulk random ionic polymers of $f_c = 0.1$ and $l_B = 5.6$. Larger clusters are formed at lower temperatures. (b) Temporal evolution of the number of clusters n_c inside the simulation box (in the production run) for systems of $f_c = 0.1$ at different l_B and T. The variation of n_c decreases as l_B increases and T decreases.

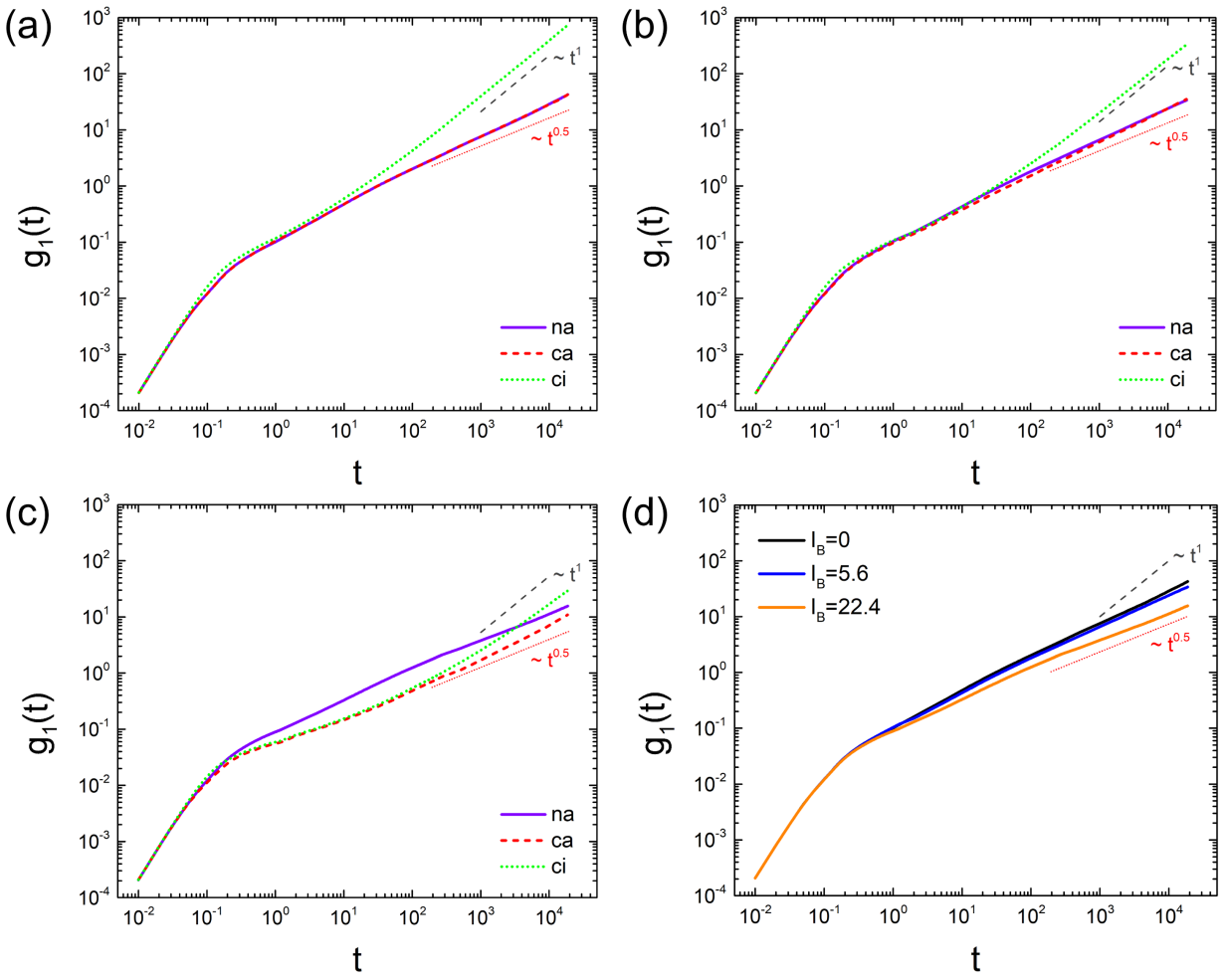

Figure S9: Mean-square displacement (MSD) profiles of neutral beads (na), charged beads (ca), and counterions (ci) in bulk random ionic polymers at $f_c = 0.1$ and $T = 0.7$ for: (a) $l_B = 0$, (b) $l_B = 5.6$, and (c) $l_B = 22.4$. (d) Comparison of na MSDs in the three systems.

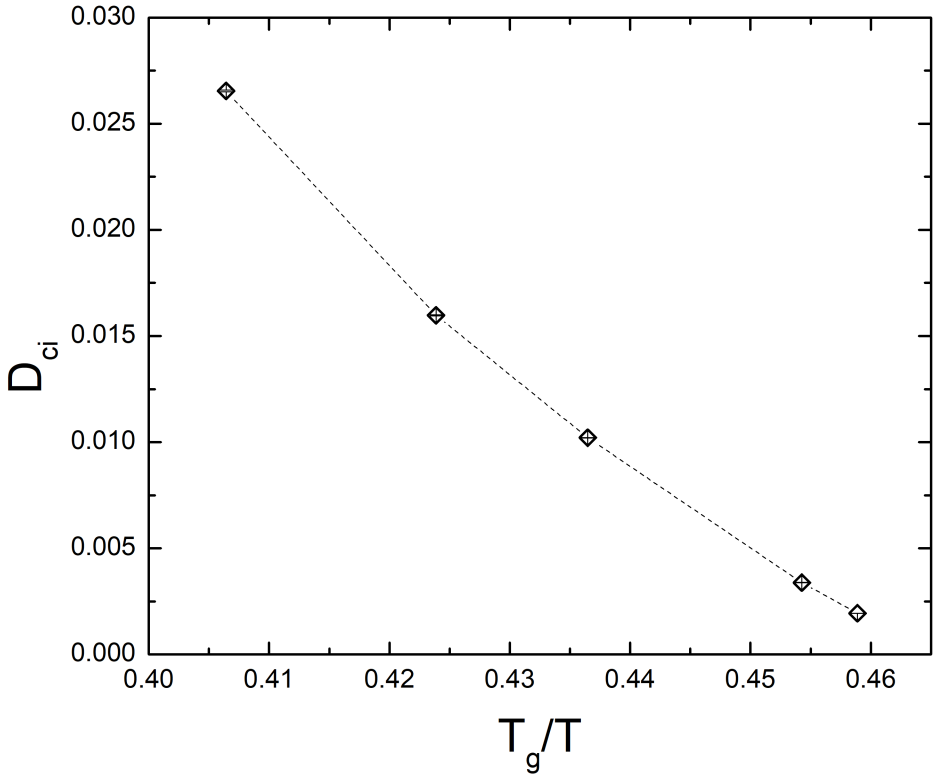

Figure S10: Plot of counterion diffusivity, $D_{\rm ci}$, versus T_g/T for bulk random ionic polymers of different l_B at $T = 1.0$.

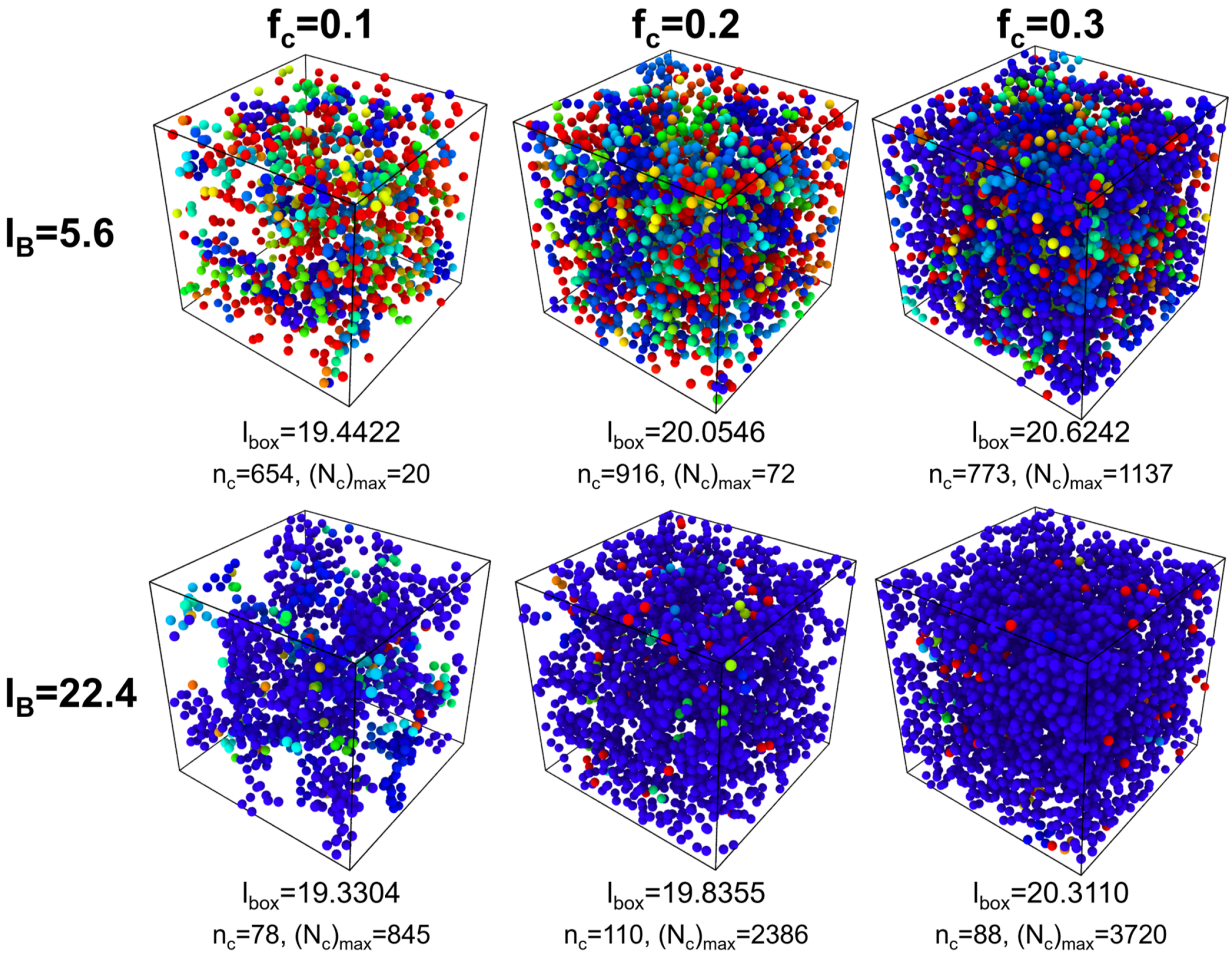

Figure S11: Snapshots of ionic association inside the simulation box of bulk random ionic polymers for different charge fraction f_c and Bjerrum length l_B at $T = 0.7$. The cubic box side length $l_{\rm box}$, total number of clusters n_c, and the maximum cluster size in the snapshot $(N_c)_{\rm max}$ are shown. The clusters are color-coded differently for visualization, where the cluster size reduces from blue to red (with red beads representing free particles, i.e., $N_c = 1$).

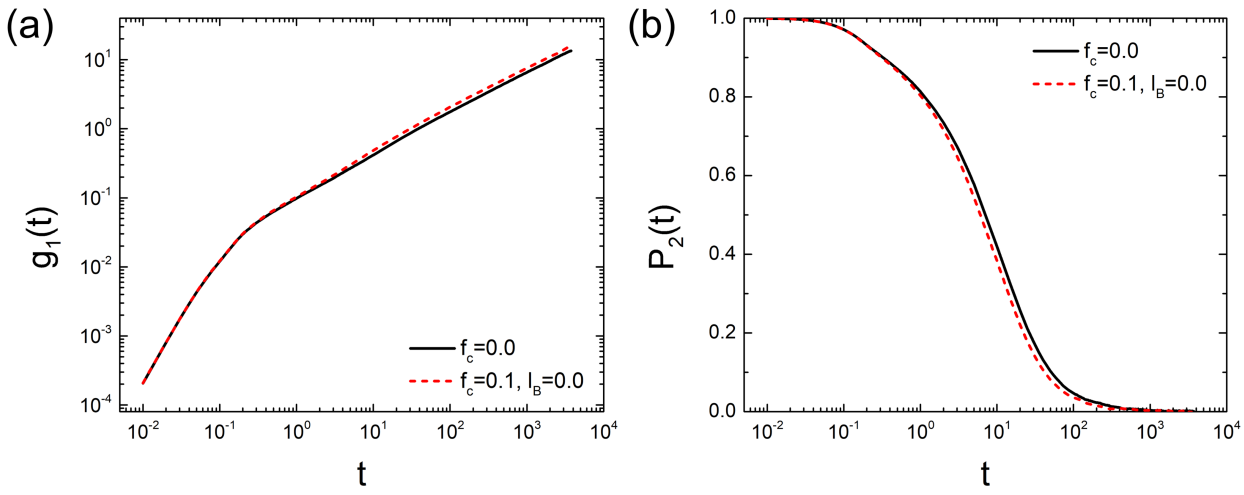

Figure S12: Comparisons of (a) mean-square displacement $g_1(t)$ of polymer beads and (b) bond orientational autocorrelation function $P_2(t)$ of all bonds in neat neutral polymers ($f_c = 0.0$) and ionic polymers of $f_c = 0.1$ and $l_B = 0.0$ at $T = 0.7$. The plots show smaller MSD and slower decay of $P_2(t)$ in the system of $f_c = 0.0$, suggesting a higher T_g compared to the system of $f_c = 0.1$ and $l_B = 0.0$.

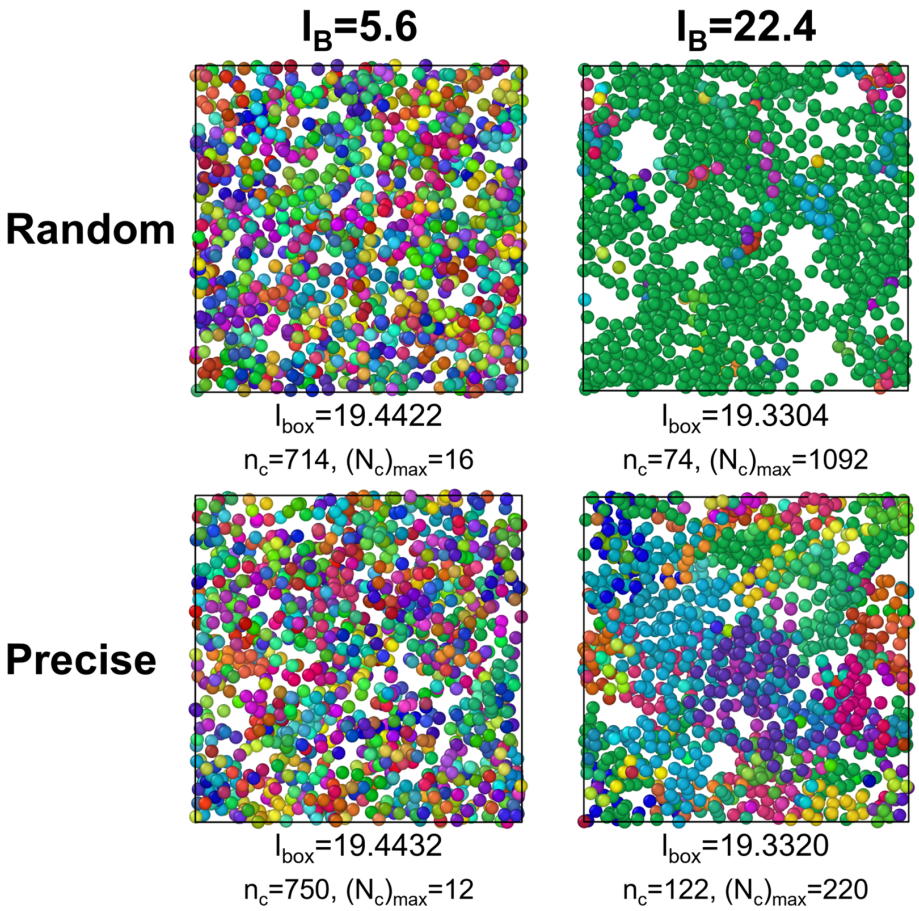

Figure S13: Snapshots (top view) of ionic association in random and precise ionic polymers of $f_c = 0.1$ at $T = 0.7$ for $l_B = 5.6$ and 22.4 (different frames of the random cases are adopted in contrast to corresponding systems in Figure S11). The clusters are color-coded differently, and the cubic box side length l_{box}, total number of clusters n_c, and the maximum cluster size in the snapshot $(N_c)_{\mathrm{max}}$ are shown.

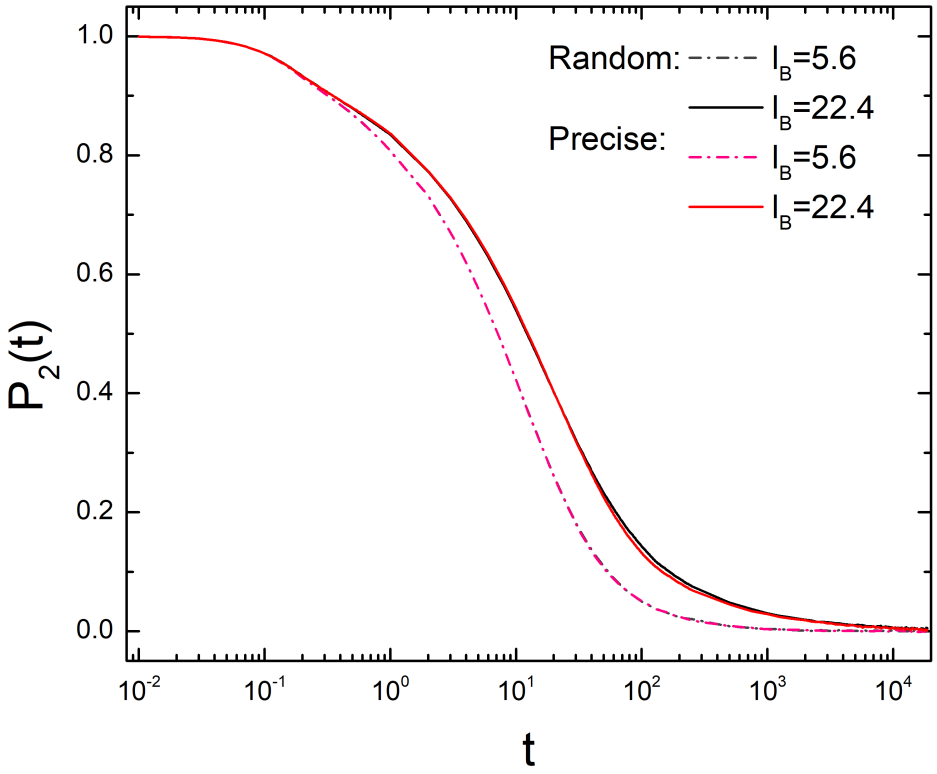

Figure S14: Bond orientational autocorrelation function $P_2(t)$ of all bonds in random and precise ionic polymers of $f_c = 0.1$ and $T = 0.7$ at $l_B = 5.6$ and 22.4.

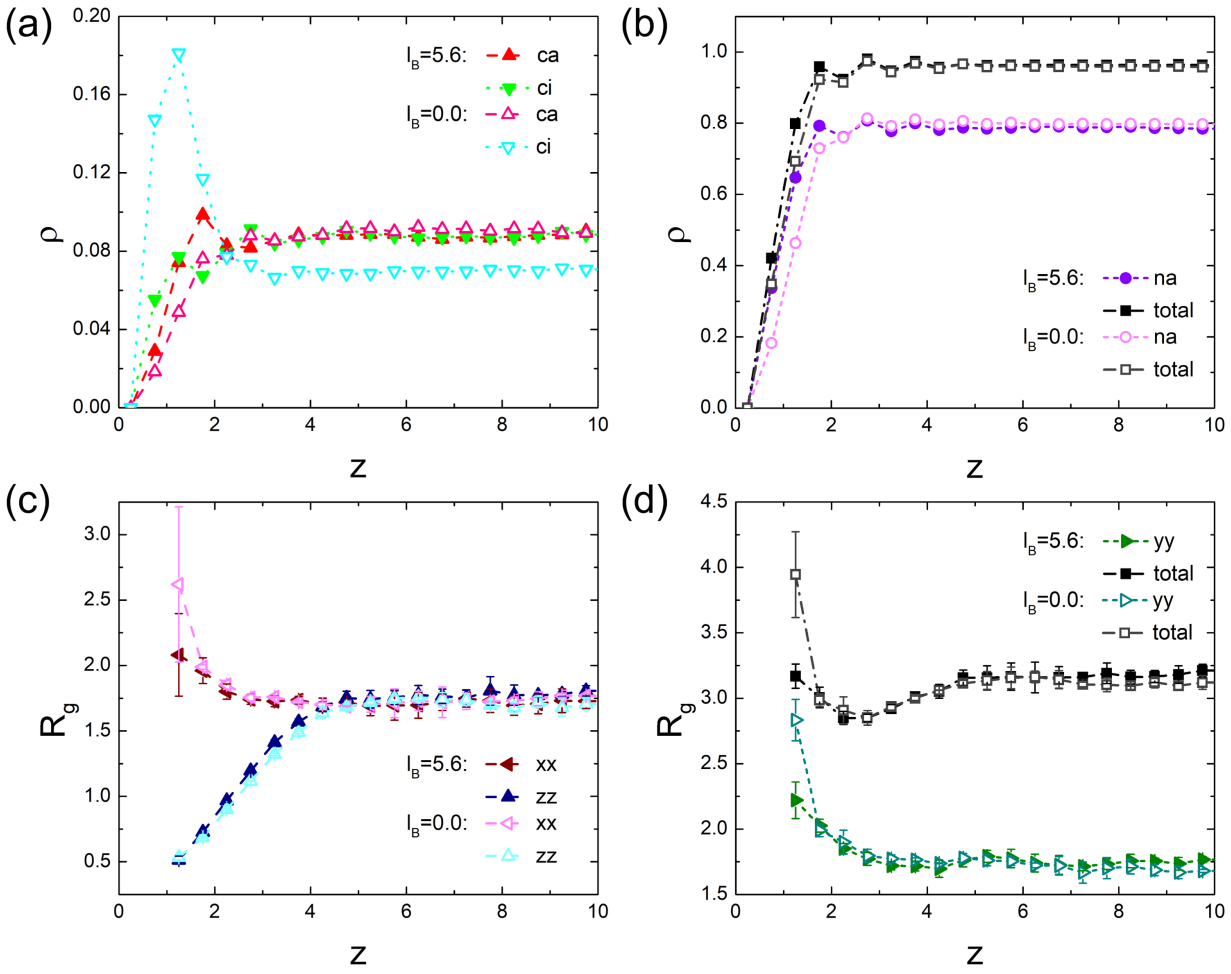

Figure S15: Comparisons between random ionic polymer thin films of $l_B = 5.6$ and 0.0 at $f_c = 0.1$, $T = 0.7$, and $h = 20$: (a) Profiles of number density ρ for ca and ci near the wall; (b) ρ of na and total beads; (c) xx and zz components of layer-resolved R_g profiles; and (d) yy components and total R_g.

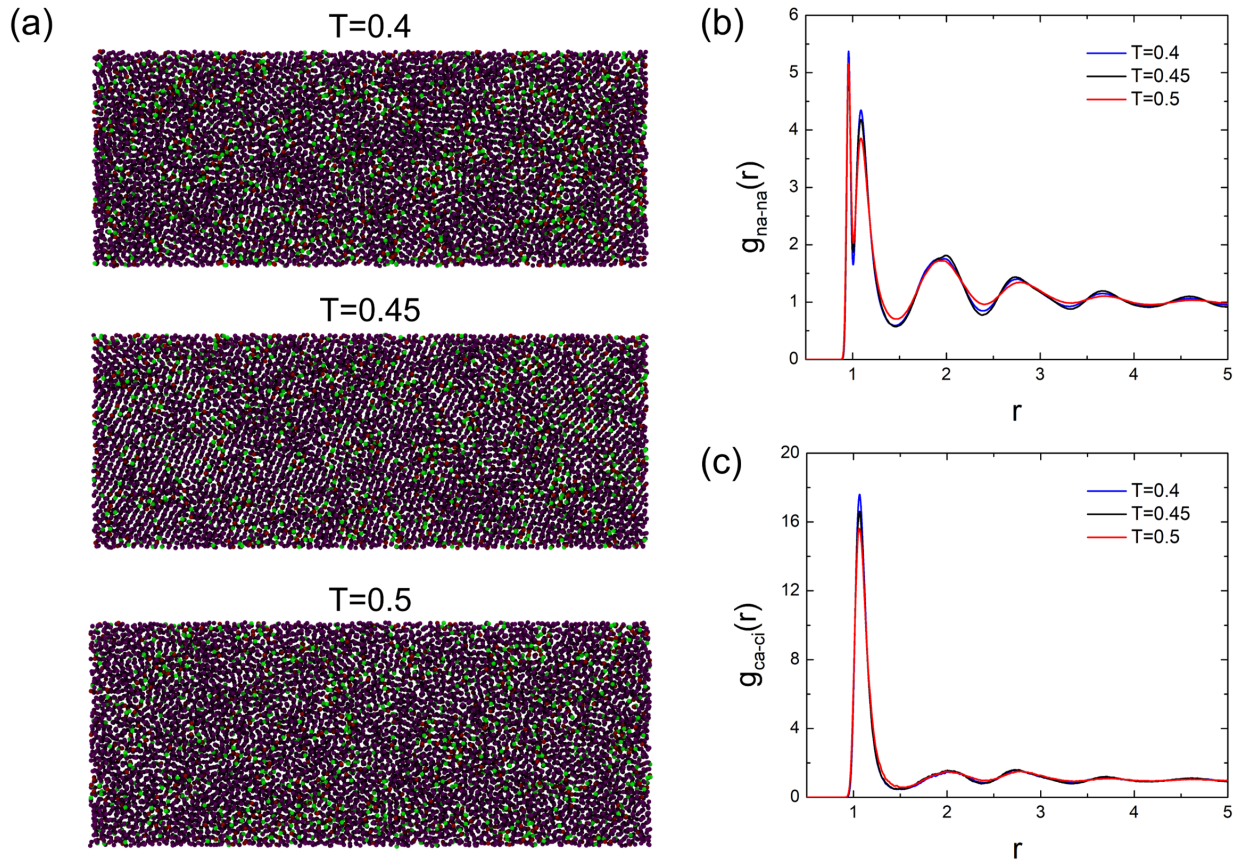

Figure S16: (a) Top view of system configuration at $T = 0.4$, 0.45, and 0.5 for thin films of random ionic polymers at $f_c = 0.1$, $l_B = 5.6$, and $h = 6$. Corresponding radial distribution functions of (b) $g_{\text{na-na}}(r)$ and (c) $g_{\text{ca-ci}}(r)$. In particular, $g_{\text{na-na}}(r)$ of $T = 0.45$ shows stronger high order peaks due to the formation of more ordered packing structures compared to the other two temperatures.

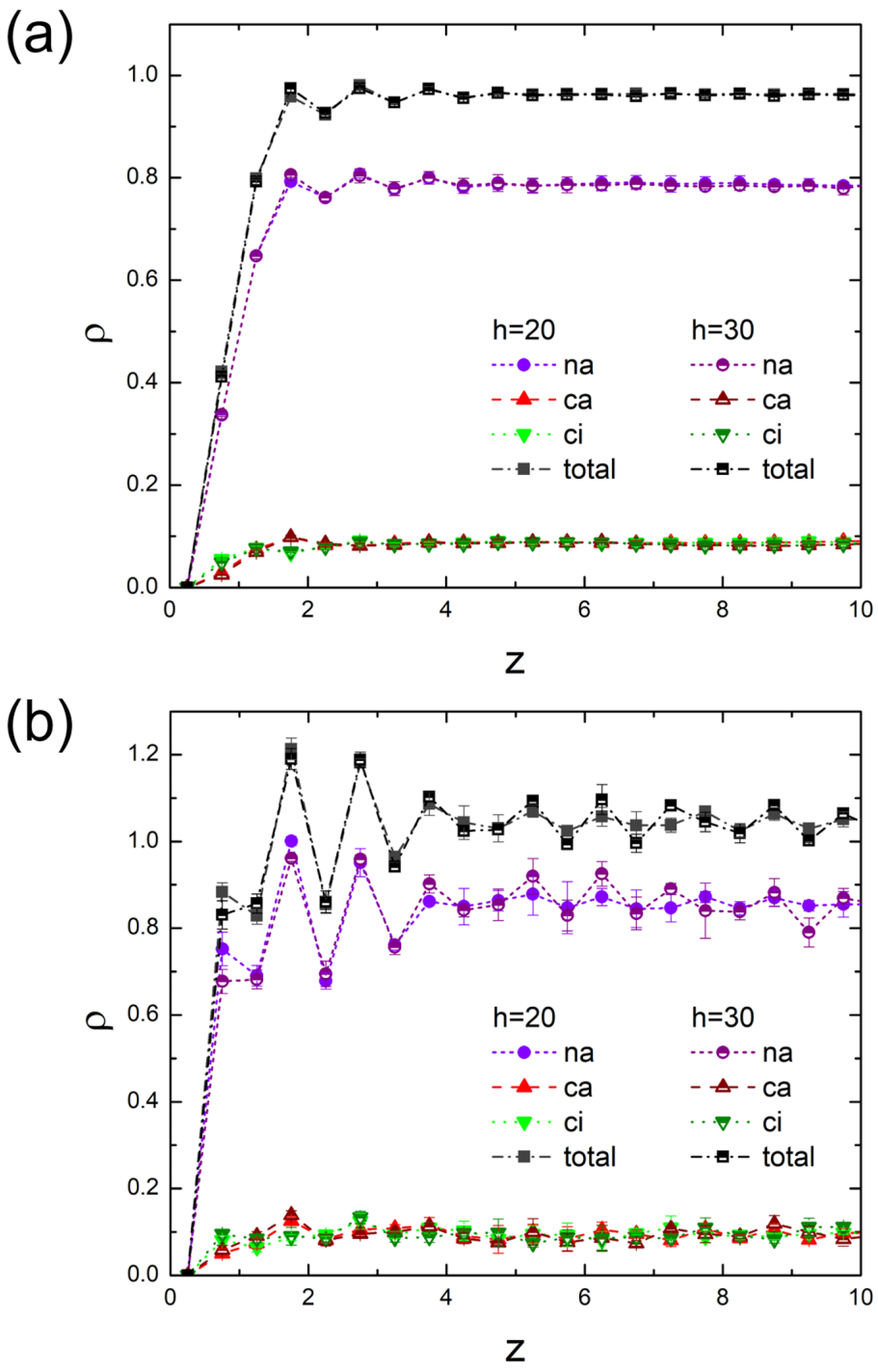

Figure S17: Comparisons of density profiles near the wall in thin films of $h = 20$ and 30 for random ionic polymers with $f_c = 0.1$ and $l_B = 5.6$ at (a) $T = 0.7$ (melt) and (b) $T = 0.4$ (glass).

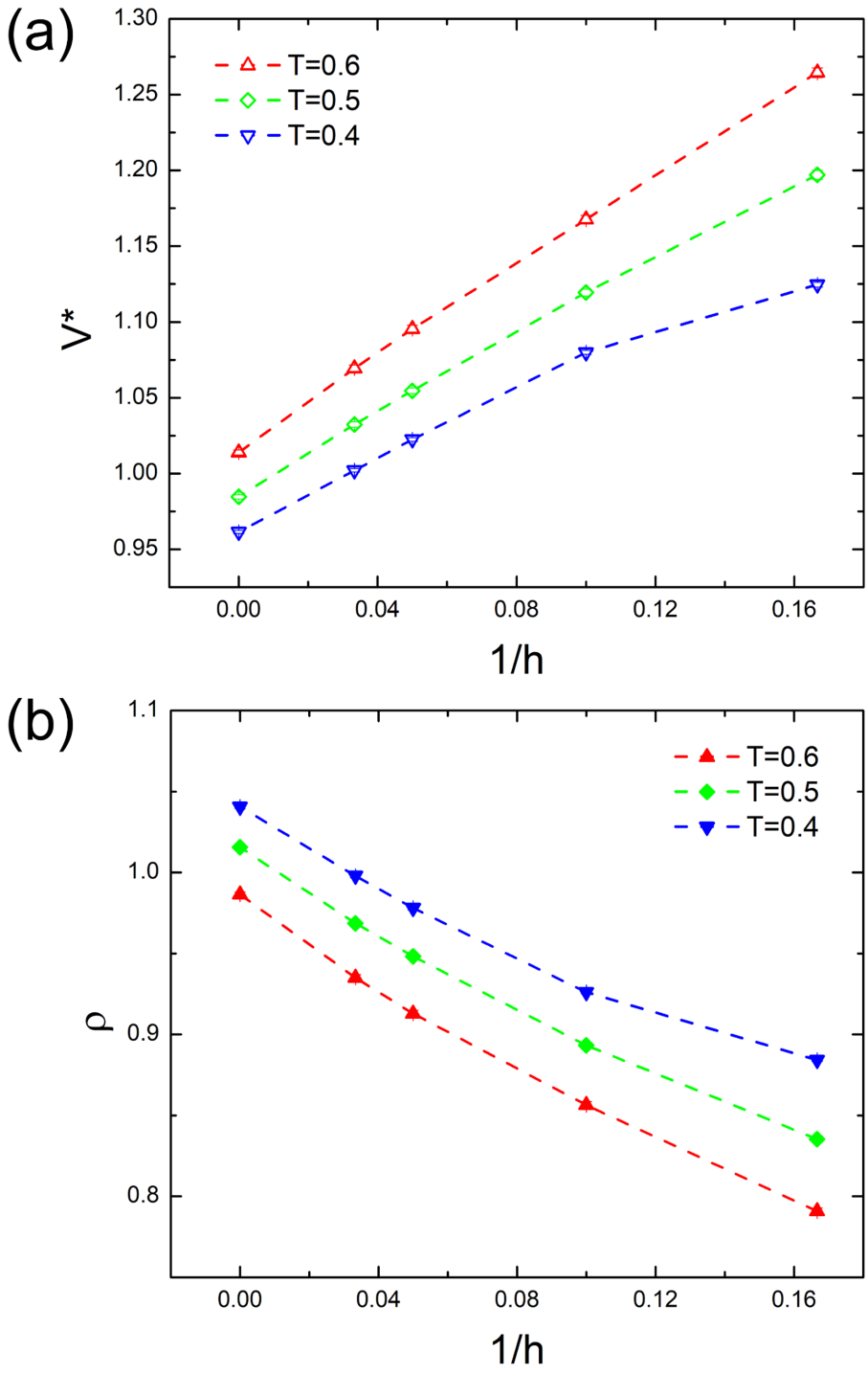

Figure S18: Plots of (a) specific volume V^* and (b) number density ρ against $1/h$ for random ionic polymer films of $f_c = 0.1$ and $l_B = 5.6$ at different temperatures.

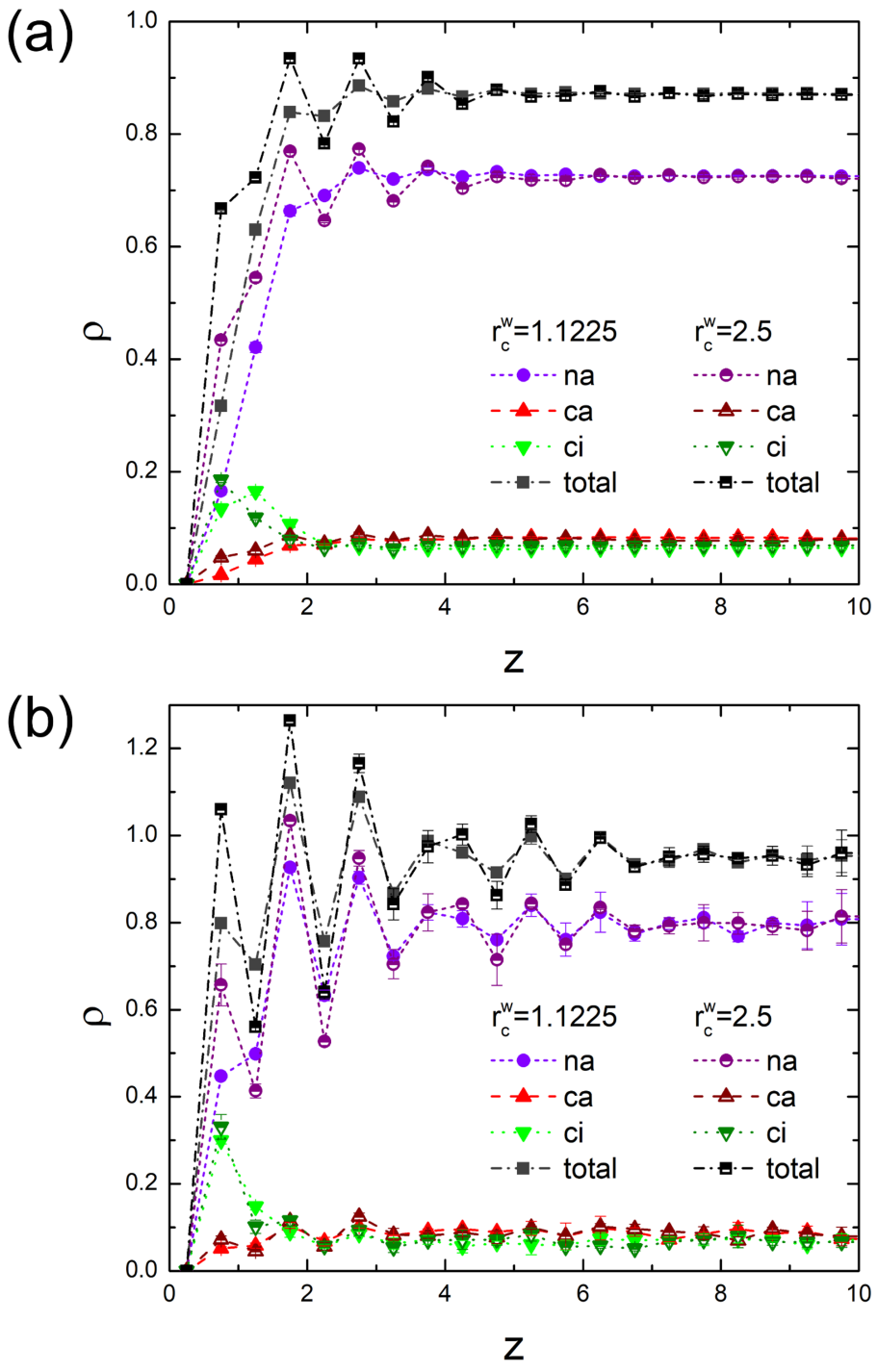

Figure S19: Comparisons of density profiles near the wall in thin films of $h = 20$ for neutral systems of $f_c = 0.1$ and $l_B = 0$ with different wall affinities at (a) $T = 0.7$ (melt) and (b) $T = 0.4$ (glass). Increasing the cut-off distance from $r_c^w = 1.1225$ to 2.5 increases the attraction well depth from 0.394ϵ to 0.990ϵ, enhancing the wall affinity with particles.